Effect of Nitrogen Doping on the Mechanical Properties of Carbon Nanotubes

Yogeeswaran Ganesan, Cheng Peng, Yang Lu, Lijie Ci, Anchal Srivastava, Pulickel M. Ajayan, and Jun Lou*

Department of Mechanical Engineering and Materials Science, Rice University, 6100 Main Street, Houston, Texas 77006, United States

Since the discovery of carbon nanotubes (CNTs) by Iijima in 1991, a number of potential applications for these remarkable materials have been envisioned. One of the most promising uses for these nanomaterials is as reinforcements for high strength/stiffness/toughness composites. This is because their mechanical properties are considerably better than those of conventional fibrous materials. Theoretical predictions show that CNTs must possess ultra-high strengths, as high as 300 GPa for single walled carbon nanotubes (SWNTs),[1] owing to the strength of the sp^2 C—C bonds, considered to be the strongest of all chemical bonds. Experimental studies, on the other hand, have reported tensile strength values for individual MWNTs that vary between 30—110[2,3] and 13—53 GPa[4] for SWNTs. Lower than expected values of measured strength can be attributed to the presence of defects in their structure introduced during purification, sonication, or due to electron beam induced reactions between the tubes and residual water within an electron microscope chamber.[5] Also, it is well-known that the mode of CNT synthesis plays an important role in determining the nature and distribution of defects with catalytic chemical vapor deposition (CVD) grown nanotubes having a more defect laden structure when compared to nanotubes grown via other techniques such as laser vaporization and arc discharge (AD).

Owing to their small size and the magnitude of the forces and deformation involved, the mechanical characterization of individual SWNTs via direct techniques such as tensile testing is considered extremely challenging and no reports on such experiments exist in literature. As with regard to individual MWNTs, a number of indirect as

ABSTRACT We report on the usage of a simple microfabricated device that works in conjunction with a quantitative Nanoindenter within a scanning electron microscope (SEM) chamber, for the *in situ* quantitative tensile testing of individual catalytically grown pristine and nitrogen-doped multiwall carbon nanotubes (MWNTs). The two types of MWNTs were found to possess similar strengths but different load-bearing abilities owing to the differences in their wall structures. Also, stress *versus* strain curves and fracture surfaces showed that while the pristine MWNTs deform and fail in a brittle fashion, the nitrogen-doped MWNTs deform plastically to varying degrees prior to failure. High resolution transmission electron microscope (TEM) images of the nitrogen-doped MWNT fracture specimens showed the presence of regions of reduced cross-section areas and kinks in close proximity to the fracture surfaces. The presence of nitrogen atoms in the graphitic sheets was assumed to have led to the formation of kinks whose motion induced by straining could have resulted in the plastic deformation of the carbon nanotubes.

KEYWORDS: nitrogen doping · multiwall carbon nanotube · *in situ* tensile testing · plasticity · fracture

well as direct measurements of the mechanical properties (including tensile strength) that involved the use of MEMS-based platforms,[3,6] atomic force microscopy,[2,7] *via* lateral bending of suspended nanotubes,[8–10] and dynamic vibration analysis,[11] among others, have been reported in the past. MEMS-based tensile testing techniques have a number of advantages over indirect mechanical techniques such as dynamic vibration analysis and AFM-based lateral bending.[12] Some of these advantages include their ability to provide *in situ* imaging of deformation and obtain stress *versus* strain curves for the specimens tested. However, most of the aforementioned MEMS based studies have focused on high quality nearly defect free arc discharge grown MWNTs; such MWNTs have been found to possess excellent mechanical properties and their deformation usually involves only a single (outermost) load-bearing shell. Little is known, however, about the mechanical strength, nature of intershell load transfer, and failure
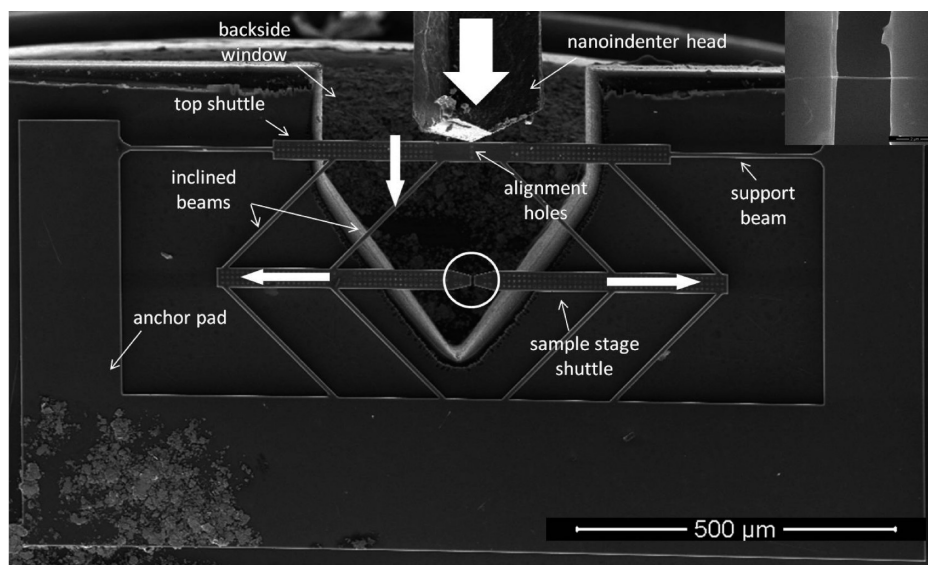
Figure 1. SEM image of the novel microfabricated device: block arrows show the direction of movement of the indenter tip and the shuttles during the experiment; (Inset) close up view of circled region showing an MWNT specimen across the sample stage shuttle gap. The scale bar in the inset reads 2 μm.

mechanisms associated with MWNTs grown catalytically *via* chemical vapor deposition even though these materials are routinely used for research and commercial applications. Recently we developed a simple microfabricated device (see Figure 1) that works in conjunction with a quantitative nanoindenter within an SEM/TEM chamber, which can be used to perform *in situ* tensile tests on 1-D nanoscale specimens.[13,14] The device was used to probe the mechanical properties of individual pristine MWNTs and that of nitrogen-doped MWNTs (CN$_x$ nanotubes), grown catalytically by uniaxial tensile testing, *in situ*, within an SEM chamber.

RESULTS AND DISCUSSION

Strength and Load-Bearing Abilities. It is well established that, when defect-free MWNTs are subject to tensile loading, only the outermost wall of each tube can be considered to be load-bearing. Such MWNTs fail *via* a "sword in sheath" mechanism, with the inner walls experiencing a pullout after failure of the load-bearing wall.[2] On the other hand, in the case of catalytically grown MWNTs such as the ones used in our experiments, the presence of a large density of vacancies, interstitials of carbon atoms, or atoms of the catalyst and dislocations can result in significant intershell cross-linking as a result of which multiple graphitic shells bear tensile loads. The occurrence of cross-linking can be confirmed by the observation of multiple wall fracture at the point of nanotube failure on a fractured specimen. B.Peng et al., for example, observed a simultaneous fracture of 3—52 shells in arc discharge grown MWNTs that were intershell cross-linked *via* electron irradiation.[3] Thus, to accurately plot the stress *versus* strain curves for the catalytically grown MWNT specimens we tested (see Figure 2), the nanotube load-bearing cross section areas were estimated *via* exami-

nation of representative fractured specimens using transmission electron microscopy (TEM). TEM images (see Supporting Information, Figure S1(a)) revealed that the pristine MWNTs possessed a nested tube structure wherein each MWNT comprised of about 100 continuous shells; the presence of arrays of internal carbon walls (compartment layers) was not obviously evident along the length of the specimens. The CN$_x$ nanotubes, on the other hand, exhibited very distinct morphologies, significantly different from the pristine MWNTs. These tubes possessed a nitrogen content of 2—3%, as determined by X-ray photoelectron spectroscopy (XPS; data not included in manuscript), and exhibited a bamboo like structure (see Supporting Information, Figure S1(b)), wherein the interior of the nanotubes contained irregularly spaced arrays of compartment layers. The CN$_x$ nanotubes we tested were each found to be made up of about 50—80 shells; while the outer 20 or so graphitic shells were continuous throughout the length of the MWNTs, the inner 30—60 shell arrays were found to combine with compartment layers without any defects, resulting in irregular reductions in the total wall thickness. It is important to note that the tube itself did not appear to be a linearly stacked line of bell cavities, a characteristic observed frequently in such nanotubes,[15,16] owing to the presence of the outer array of continuous shells. The differences in the morphologies of the inner and outer wall arrays were assumed to have arisen due to the higher nitrogen incorporation within the internal nanotube walls.[16]

In the case of all the pristine MWNTs tested, careful analysis of SEM and TEM images (see Figure 3a,c) of fracture specimens led us to the conclusion that all the shells bore the tensile load because all the graphitic shells were found to have failed in close proximity to one another. On the other hand, TEM images (see Fig-

ure 3b,d) of fractured nitrogen-doped MWNT specimens showed that the inner shell arrays that were connected to compartment layers remained intact in the regions where failure occurred. Only the outer 20 or so shells of the MWNTs were found to have failed as a result of the tensile loads. Based upon this, one could conclude that, in the case of the nitrogen-doped MWNTs, the outer shell arrays bore the bulk of the tensile loads; the inner shell arrays were subject to minimal amount of stresses, if any, during the tensile tests. The stress values plotted in Figure 4b were computed based on the assumption that only the outer continuous walls bore the tensile loads during the experiments. From stress *versus* strain curves it is evident that, while both types of nanotubes were found to possess comparable strengths, average values being 2.09 GPa (see Figure 4a and Table 1) and 1.52 GPa (see Figure 4b and Table 1) for the pristine and nitrogen-doped MWNTs, respectively, the pristine MWNTs had higher load-bearing capacities as compared to the nitrogen-doped MWNTs due to the differences in the load-bearing cross section areas. Note also that the strength values of all the MWNTs tested, while consistent with the Young's modulus measurements performed by bending[9,10] (values as low as 12 GPa were reported), were found to be considerably lower than those reported by Barber *et al.*[7] However, one must bear in mind that the high values reported in the latter manuscript were computed based on the assumption that only the outermost wall of each nanotube tested was load-bearing. Based on our analysis of fractured specimens, we believe that this might not necessarily be a reasonable assumption for the MWNT samples investigated in this study.

Brittle *versus* Plastic Behavior. Another intriguing feature observed during the course of the experiments was the fact that, while the stress *versus* strain curves for most of the pristine MWNTs tested were linear up until the point of failure, the curves for the nitrogen-doped MWNTs consistently exhibited varying degrees of nonlinearity especially at high stress levels. High resolution fracture surface images (see Figure 3d and e) of the tested nitrogen-doped MWNTs specimens clearly showed the presence of a 35−150 nm long region of reduced cross-section area that often extended beyond the amorphous carbonaceous layer that uniformly covered all the tested MWNTs. More importantly, close observation of the HR-TEM images of multiple fractured specimens clearly indicated the presence of kinks on the outer continuous wall arrays adjacent to these regions of reduced cross-section area (see Figure 3d). On the other hand, while some of the pristine MWNT stress *versus* strain curves did exhibit a certain degree of nonlinear behavior their post failure specimens were found to consistently possess relatively flat fracture surfaces (see Figure 3c) that were in the vicinity of or were embedded within the pre-existent amorphous carbonaceous layers, and no kinks were found in the proxim-
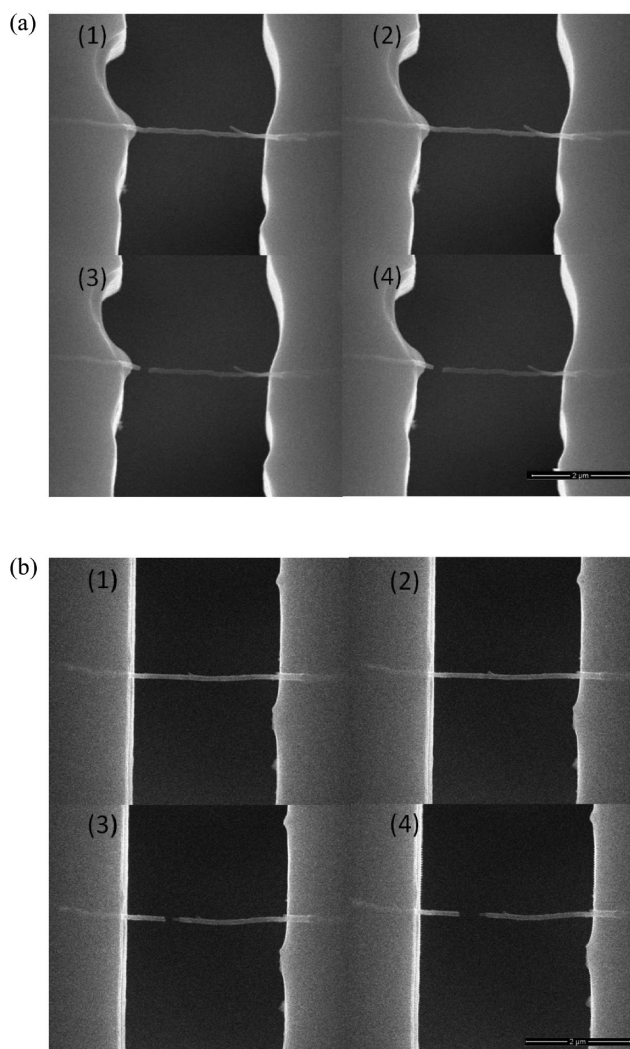
Figure 2. (a) SEM snapshots show a pristine MWNT specimen undergoing deformation under a tensile load at (1) $t = 0$, (2) $t = 4$, (3) $t = 15$, and (4) $t = 17$ s. (b) SEM snapshots show a nitrogen-doped MWNT specimen undergoing deformation under a tensile load at (1) $t = 0$, (2) $t = 1$, (3) $t = 5$, and (4) $t = 8$ s. Note that the scale bar reads 2 μm in images.

ity of the fracture surfaces (features that were consistent with brittle bond breaking mechanism of failure).

At temperatures close to 2000 °C, superplasticity has been observed in the past by Huang *et al.* in catalytically grown SWNTs,[17] and the phenomenon was attributed to the formation and motion of kinks caused by Stone-Wales defects; in fact, kink motion was found to be the universal plastic deformation mode in all nanotubes.[18] The formation of such defects in CNTs depends on a number of interdependent factors such as strain, symmetry, time, and temperature.[19] Theoretical studies have shown that that the two alternative routes of brittle bond breaking and plastic relaxation (*i.e.*, *via* kink formation and motion) are mutually competitive. At ambient temperatures, the former failure mechanism is more likely to be prevalent since kink formation requires thermal activation. However, semiempirical (PM3) and DFT-based computations have shown that
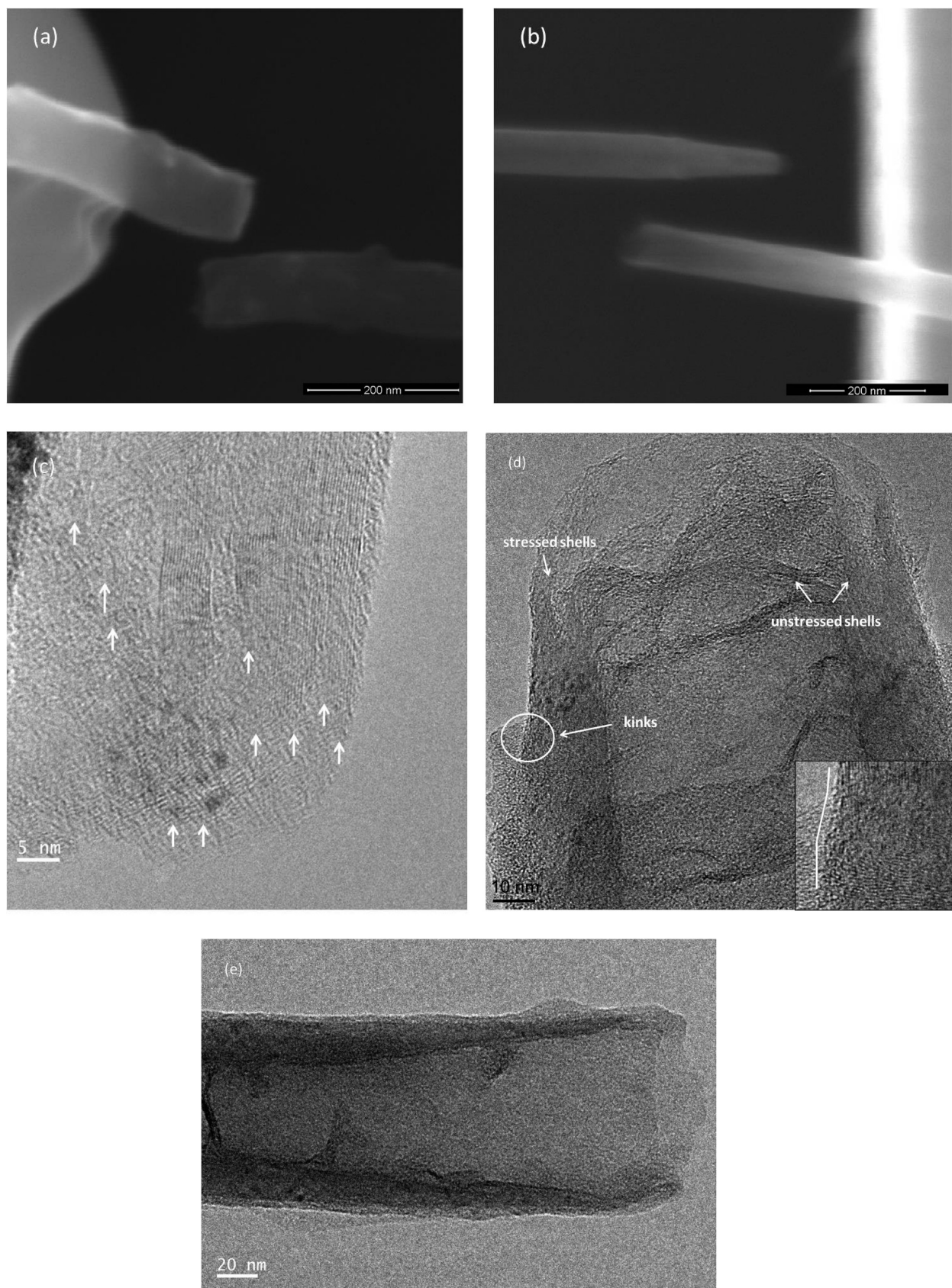
Figure 3. SEM images show a close up view of (a) a pristine MWNT fracture specimen and (b) a nitrogen-doped MWNT fracture specimen; TEM images show (c) a section of the fracture surface of a pristine MWNT, with arrows indicating the regions where wall fracture occurred and (d and e) fracture surfaces, corresponding to the left and right sections shown in (b), respectively, of a nitrogen-doped MWNT, with arrows indicating the load-bearing and the non-load-bearing walls; inset in (d) shows a close up view of a kink (circled in image) that was observed on the MWNT wall.

TABLE 1. Measured Maximum Load Borne and the Tensile Strength Values of Five Pristine and Five Nitrogen-Doped MWNTs[a]

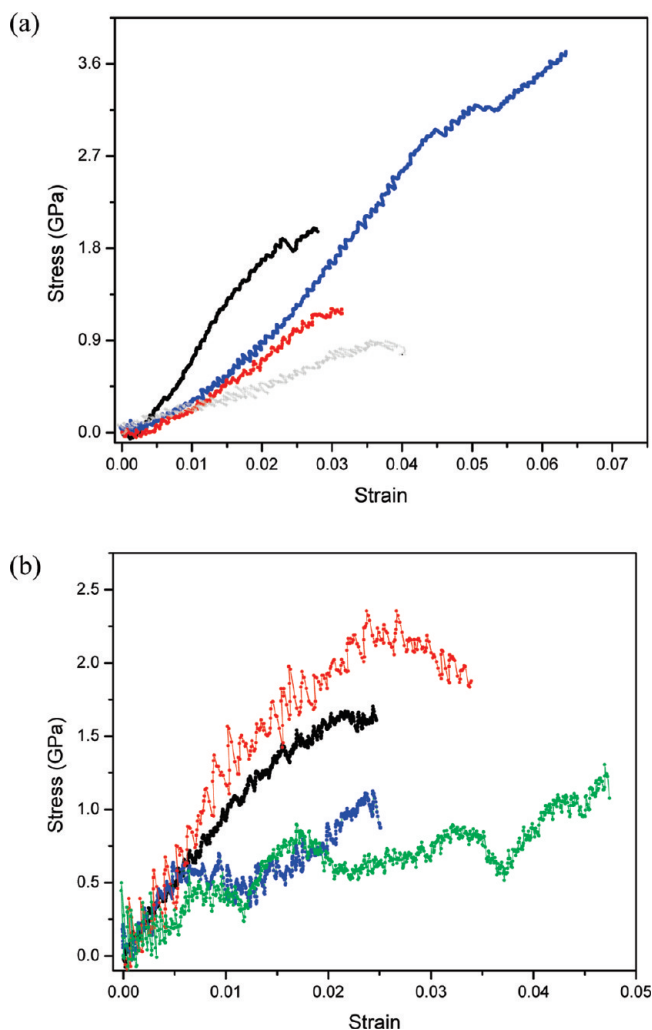| MWNT type	maximum load (nN)	tensile strength (GPa)
pristine	6873	1.20
pristine	36838	3.72
pristine	15929	1.96
pristine	11179	0.99
pristine	11654	2.80
nitrogen-doped	3953	2.33
nitrogen-doped	3409	1.61
nitrogen-doped	2120	1.13
nitrogen-doped	1829	1.23
nitrogen-doped	2557	1.32

[a]All sample diameters were in the 70—100 nm range.

the presence of nitrogen atoms can considerably reduce the activation barrier for Stone-Wales transformation in fullerenes.[20] It is, thus, possible that the plastic deformation observed in the CN_x nanotubes tested occurred due to nitrogen assisted kink formation and motion. The extent of plasticity observed in the CN_x tubes tested was considerably lesser that that observed in SWNTs[17] at high temperatures. This phenomenon can be explained by the fact that kink motion, by means of mechanisms such as dislocation climb, is more facile at high temperatures because they are dominated by the movement of vacancies and interstitials, both of which become highly active at high temperatures.

CONCLUDING REMARKS

The mechanical properties of individual catalytically grown MWNTs have thus been studied by tensile testing, *in situ*, within an SEM chamber. The two types of MWNTs tested, pristine and nitrogen-doped, were found to possess markedly different load-bearing abilities owing to the differences in their wall structures. Intershell cross-linking in the MWNTs was found to have positively contributed to their load-bearing abilities, especially in pristine MWNTs that possess about 100 nested shells. However, in nitrogen-doped MWNTs, fracture specimen analysis showed that the inner wall arrays that merged with compartment layers were non-load-bearing. Also, we discovered that while the pristine MWNTs fail *via* a brittle bond-breaking mechanism, the nitrogen-doped MWNTs exhibited a certain degree of plastic behavior before failure. The repeated observation of kinks in the vicinity of the fractured surfaces led us

Figure 4. Engineering stress *versus* strain curves for (a) four pristine MWNT specimens and (b) four nitrogen-doped MWNT specimens.

to the conclusion that the plasticity observed in these tubes was a result of kink motion. The presence of nitrogen in the graphitic sheets that formed the nanotubes was assumed to have catalyzed the formation of kinks in these tubes. Based on our findings, we assert that bamboo-like MWNTs, synthesized by nitrogen doping, can exhibit a certain degree of ductility at room temperature. Further investigations to better understand these materials are necessary as they could potentially be used as reinforcements for high toughness composite applications.

METHODS

The microfabricated device (see Figure 1) used to perform the tensile experiments consists of a pair of movable (sample stage) shuttles that are attached to a top shuttle *via* inclined free-standing beams. Its actuation involves the usage of a nanoindenter that applies a lateral load on the top shuttle of the device; four sets of inclined symmetrical beams transform the

motion of the top shuttle into a two-dimensional translation of the sample stage shuttles and ensures that the stress applied on a specimen mounted across the sample stage shuttles is purely tensile. The stress *versus* strain curve for each specimen can subsequently be extracted from its corresponding nanoindenter load *versus* displacement curve either using conversion factors obtained *via* simple response subtraction calculations and im-

age correlation analysis. Device fabrication, using standard photolithographic techniques, has been described in detail earlier.[14] Its use for testing the aforementioned samples is advantageous for two reasons. (a) It allows the application and measurement of forces with nano-Newton resolution and measurement of local mechanical deformation independently and with nanometer resolution (this is because the force and displacement resolution of the devices are dictated by that of the nanoindenter *viz.* 69.4 nanonewtons and 8.675 Å, respectively). (b) Also, most catalytically grown MWNTs are curved to a certain degree; hence, the samples would be required to be pulled apart to a certain extent before any load application can occur. The use of the technique is advantageous because a clear shift in the indenter load *versus* displacement curve occurs at the point at which load application on the specimen begins (see Supporting Information, Figure F1).

Pristine MWNT specimens were grown on bare quartz substrates by injecting a mixture of 20 mg/mL of ferrocene ((C_5H_5)$_2$Fe) in xylene (C_8H_{10}) solution into a two-stage thermal CVD reactor consisting of a low temperature (200 °C) preheater followed by a higher temperature main reactor (775 °C). A similar spray pyrolysis technique was also used to synthesize the CN_x nanotubes wherein a mixture of xylene and acetonitrile (CH_3CN) acted as the carbon/nitrogen source. Basically, a 1 g ferrocene dissolved in a 75 mL of xylene + 25 mL of acetonitrile solution mixture was injected into a quartz tube that was held at 900 °C. In both cases, a hydrogen/argon mixture was used as the carrier gas.

Sample mounting was accomplished *via* the following procedure. A portion of each sample stage shuttle was first coated with a thin layer of epoxy (HARDMAN Water-Clear Epoxy). A droplet from a sonicated suspension of the MWNTs in toluene was deposited onto a Si wafer coated with a 5 nm thick layer of titanium. Individual MWNTs, that were about 10 um in length and 70−100 nm in diameter and, hence, visible under an optical microscope, were subsequently picked up and placed across the shuttles using micromanipulators housed within a probe station (The Micromanipulator Co., Carson City, NV). The epoxy layer, upon hardening, acts as a clamp for the tensile specimens. The use of epoxy was favored over e-beam induced carbon deposition methods (EBID) because it has been known to reduce the probability of nanotube slippage and debonding from the sample stage shuttles.[21] E-beam assisted Pt deposition was also considered unsuitable for sample clamping because it often causes the formation of a Pt sheath around the specimen, thus, reducing the accuracy of the stress *versus* strain curves obtained. The gauge length of the specimens, that is, the distance between the clamping points, were ascertained by observation of the side profile of the samples across the sample stage gap under a SEM.

The tensile experiments (see Figure 2) were performed within a SEM (FEI Quanta 400 high resolution field emission scanning electron microscope, FEI company, Hillsboro, Oregon) equipped with an InSEM Indenter (AGILENT Technologies, Oak Ridge, Tennessee) system. A blunt berkovich nanoindenter tip was used for load application. The nanoindenter tip was first aligned with the top shuttle of the device to make sure that the sample stage shuttles moved symmetrically. This was done with the help of alignment holes that had been incorporated in the device design. Once this was done, the electron beam was focused on the nanotube specimens to monitor their deformation and fracture in real time. The experiments were conducted at an indenter tip displacement rate of ~10 nm/s (corresponds to a strain rate of approximately 0.002 s^{-1}), with the load *versus* displacement data being collected at a rate of 25 Hz. The maximum load applied on the device varied between 0.1 and 0.5 mN. Once this value was reached, the load was held constant for 0.5 s. This was followed by an unloading step at an aforementioned displacement rate. A thermal drift correction hold step (see SI, Figure S2) was performed at about 1% of the maximum applied load for about 50 s in order to account for small amounts of thermal expansion or contraction in the test material and indentation equipment. A select number of samples tested were analyzed post-mortem within a high resolution transmission electron microscope (JEM 2100F HR-TEM) chamber. In those

cases, the devices that were used to perform the tensile tests were first separated from the substrate by etching away sections of their inclined beams using a focused ion beam (FEI Strata DB 235, FEI corp.). A micromanipulator probe was subsequently used to place the devices, laden with the fractured specimens, onto TEM grids for imaging.

REFERENCES AND NOTES

1. Kelly, B. T. *Physics of Graphite*; Applied Science: London and New Jersey, 1981; p 477.
2. Yu, M. F.; Lourie, O.; Dyer, M. J.; Moloni, K.; Kelly, T. F.; Ruoff, R. S. Strength and Breaking Mechanism of Multiwalled Carbon Nanotubes Under Tensile Load. *Science* **2000**, *287*, 637–640.
3. Peng, B.; Locascio, M.; Zapol, P.; Li, S.; Mielke, S. L.; Schatz, G. C.; Espinosa, H. D. Measurements of Near-Ultimate Strength for Multiwalled Carbon Nanotubes and Irradiation-Induced Crosslinking Improvements. *Nat. Nanotechnol.* **2008**, *3*, 626–631.
4. Yu, M. F.; Files, B. S.; Arepalli, S.; Ruoff, R. S. Tensile Loading of Ropes of Single Wall Carbon Nanotubes and Their Mechanical Properties. *Phys. Rev. Lett.* **2000**, *84*, 5552–5555.
5. Mølhave, K.; Gudnason, S. B.; Pedersen, A. T.; Clausen, C. H.; Horsewell, A.; Bøggild, P. Electron Irradiation-Induced Destruction of Carbon Nanotubes in Electron Microscopes. *Uttramicroscopy* **2007**, *108*, 215–217.
6. Demczyk, B. G.; Wang, Y. M.; Cumings, J.; Hetmana, M.; Hana, W.; Zettl, A.; Ritchie, R. O. Direct Mechanical Measurement of the Tensile Strength and Elastic Modulus of Multiwalled Carbon Nanotubes. *Mater. Sci. Eng. A* **2002**, *334*, 173–178.
7. Barber, A. H.; Kaplan-Ashiri, I.; Cohen, S. R.; Tenne, R.; Wagner, H. D. Stochastic Strength of Nanotubes: An Appraisal of Available Data. *Compos. Sci. Technol.* **2005**, *65*, 2380–2384.
8. Wong, E. W.; Sheehan, P. E.; Lieber, C. M. Nanobeam Mechanics: Elasticity, Strength, and Toughness of Nanorods and Nanotubes. *Science* **1997**, *277*, 1971–1975.
9. Lukic, B.; Seo, J. W.; Couteau, E.; Lee, K.; Gradecak, S.; Berkecz, R.; Hernadi, K.; Delpeux, S.; Cacciaguerra, T.; Beguin, F.; et al. Elastic Modulus of Multi-Walled Carbon Nanotubes Produced by Catalytic Chemical Vapor Deposition. *Appl. Phys. A: Mater. Sci. Process.* **2005**, *80*, 695–700.
10. Salvetat, J. P.; Kulik, A. J.; Bonard, J. M.; Briggs, G. A. D.; Stöckli, T; Metenier, K; Bonnamy, S.; Beguin, F.; Burnham, N. A.; Forro, L. Elastic Modulus of Ordered and Disordered Multiwalled Carbon Nanotubes. *Adv. Mater.* **1999**, *11*, 161–165.
11. Poncharal, P.; Wang, Z. L.; Ugarte, D.; de Heer, W. A. Electrostatic Deflections and Electromechanical Resonances of Carbon Nanotubes. *Science* **1999**, *283*, 1513–1516.
12. Li, X. D.; Chasiotis, I.; Kitamura, T. In Situ Scanning Probe Microscopy Nanomechanical Testing. *MRS Bull.* **2010**, *35*, 361−367.
13. Lu, Y.; Ganesan, Y.; Lou, J. A Multi-Step Method for In Situ Mechanical Characterization of 1-D Nanostructures Using a Novel Micromechanical Device. *Exp. Mech.* **2010**, *50*, 47–54.

14. Ganesan, Y.; Lu, Y.; Peng, C.; Lu, H.; Ballarini, R.; Lou, J. Development and Application of a Novel Microfabricated Device for the In Situ Tensile Testing of 1-D Nanomaterials. *JMEMS* **2010**, *19*, 675–682.

15. Jang, J. W.; Lee, C. E.; Lyu, S. C.; Lee, T. J.; Lee, C. J. Structural Study of Nitrogen-Doping Effects in Bamboo-Shaped Multiwalled Carbon Nanotubes. *Appl. Phys. Lett.* **2004**, *84*, 2877–2879.

16. Ewels, C. P.; Glerup, M. Nitrogen Doping in Carbon Nanotubes. *J. Nanosci. Nanotechnol.* **2005**, *5*, 1345–1363.

17. Huang, J. Y.; Chen, S.; Wang, Z. Q.; Kempa, K.; Wang, Y. M.; Jo, S. H.; Chen, J.; Dresselhaus, M. S.; Ren, Z. F. Superplastic Carbon Nanotubes. *Nature* **2006**, *439*, 281.

18. Huang, J. Y.; Chen, S.; Ren, Z. F.; Wang, Z. Q.; Wang, D. Z.; Vaziri, M.; Suo, Z.; Chen, G.; Dresselhaus, M. S. Kink Formation and Motion in Carbon Nanotubes at High Temperatures. *Phys. Rev. Lett.* **2006**, *97*, 075501-1–075501-4.

19. Dumitrica, T.; Hua, M.; Yakobson, B. I. Symmetry-, Time-, and Temperature-Dependent Strength of Carbon Nanotubes. *Proc. Natl. Acad. Sci. U.S.A.* **2006**, *103*, 6105–6109.

20. Slanina, Z.; Zhao, X.; Uhlik, F.; Ozawa, M.; Osawa, E. Computational Modeling of the Elemental Catalysis in the Stone-Wales Fullerene Rearrangements. *J. Organomet. Chem.* **2000**, *599*, 57–61.

21. Barber, A. H.; Andrews, R.; Schadler, L. S.; Wagner, H. D. On the Tensile Strength Distribution of Multiwalled Carbon Nanotubes. *Appl. Phys. Lett.* **2005**, *87*, 203106-1–203106-3.

ARTICLE